Vol. 32 (2001) ACTA PHYSICA POLONICA B No 3

NUCLEAR PROPERTIES IN $f_{7/2}$ SHELL*

Daniel R. Napoli

INFN — Laboratori Nazionali di Legnaro, Italia

(Received November 28, 2000)

A review of some results we have recently obtained for medium-light nuclei is reported, with particular stress on the nuclear properties we have studied and what we have learned from these experiments. To illustrate these features of $f_{7/2}$-shell nuclei, we present some examples on rotational bands in even–even and odd–odd nuclei, backbending and band termination phenomena, intruder bands and shape coexistence and, finally, analogue bands in $T = 1$ mirror nuclei.

PACS numbers: 21.10.Hw, 21.10.Re, 21.60.Cs

1. Introduction

Nuclei along the $N = Z$ line are of special interest because they allow to study particular symmetries between protons and neutrons by exploring the proton–neutron pairing correlation, $T = 0$ and $T = 1$ bands in odd–odd $N = Z$ nuclei, isospin symmetry in mirror nuclei and isobaric multiplets.

Near the middle of the $f_{7/2}$ shell, these nuclei show strong deformation at low spin and therefore we observe rotational g.s. bands in most of the cases. At high spin, some symmetries can be explored at high rotational frequency. It is important to remember that although the angular momentum which can be transferred to these relatively light nuclei is not very high, the angular frequencies that these nuclei can reach in a normal low energy nuclear reaction ($E_{\rm lab} \approx 5\,{\rm MeV}/A$) are extremely high. Thus Coriolis and centrifugal forces play a very important role and effects such as changes of shape, band termination and backbending phenomena are clearly manifested at high spin.

Even if the nuclei we are studying are not very far from stability, a very efficient detection system is needed to study them at high spin. In first place because the angular momentum that can be transferred to the compound

* Presented at the XXXV Zakopane School of Physics "Trends in Nuclear Physics", Zakopane, Poland, September 5–13, 2000.

nucleus in a fusion–evaporation reaction is restricted due to the light mass of the reaction partners, in addition the transition energies become large (2–5 MeV) at the high spin regime and finally, we have to deal with high recoil velocities as it is for the symmetric reaction that we have the higher transferred angular momentum to the compound system.

Due to the low Coulomb barrier, charged particles are evaporated with high probability. Therefore, the fusion cross section fractionates in a large number of competing channels and the evaporation, specially of the heavier particles, changes the recoil direction and produces a large spread in recoil velocity, which considerably increases the peak widths. This evaporation also reduces the probability of populating neutron deficient nuclei.

As a result of these difficulties, the detailed investigation of the high spin structure of medium-light nuclei has become experimentally feasible only in the last few years due to the advent of the new γ-ray arrays and ancillary detectors which can now simultaneously detect, with high efficiency, γ-rays and charged particles providing a powerful technique for both selecting the individual channels and for reconstructing the kinematics, that allows for an improvement in energy resolution.

Parallel progress has been made in the theoretical study of $f_{7/2}$-shell nuclei. Recent advances in large-scale and Monte Carlo shell model methods have enabled computations for these nuclei involving the full pf shell model space [1, 2]. Of particular interest have been theoretical works on ^{48}Cr [1] and ^{50}Cr [3] in which large-scale shell model have been compared with cranked Hartree–Fock–Bogoliubov. Collective nuclei in the middle of the $f_{7/2}$ shell have thus provided the opportunity for new insights into the relationship between the microscopic shell model picture of nuclei in the laboratory frame and the mean-field cranking description of the nuclear intrinsic state. In other words, in the $f_{7/2}$ shell, rotational nuclei have enough number of valence particles to develop collective motion, but this number is still accessible for an exact description with large-scale shell model. Therefore, these are unique cases in which very different treatments like collective description and spherical shell model, can be compared in the same physical system.

In the last few years, we have performed a systematic study of $f_{7/2}$ shell nuclei, in particular we have focused mainly on the $N = Z$ line. In the following sections we present some results obtained at the Legnaro National Laboratory using both γ-ray arrays, Gasp and EUROBALL combined with the charged-particle detector Isis and the Neutron Wall (only for EUROBALL), and more recently measurements performed with the on-line mass separator at GSI.

2. Rotational bands in $N = Z$ even–even nuclei

Let us take, as an example, the best rotor in the $f_{7/2}$ shell that is ^{48}Cr because it has 4 protons and 4 neutrons, the maximum number of valence particles to develop deformation, in particular, the deformation parameter, deduced from the lifetime analysis is $\beta \approx 0.28$ at low spin [4, 5].

As can be seen in Fig. 1, ^{48}Cr has a rotational g.s. band that presents a backbending around spin 12^+ and terminates at spin 16^+. Recently, we have identified with EUROBALL new positive parity states in this nucleus. Due to their non-yrast character they are very weakly populated. Another new important result concerns the negative parity band. Parity and spin assignment of the bandhead has been a matter of controversy for many years. The angular distribution of the 1674 keV linking transition is consistent with both a stretched quadrupole and a non-stretched dipole transition. On the

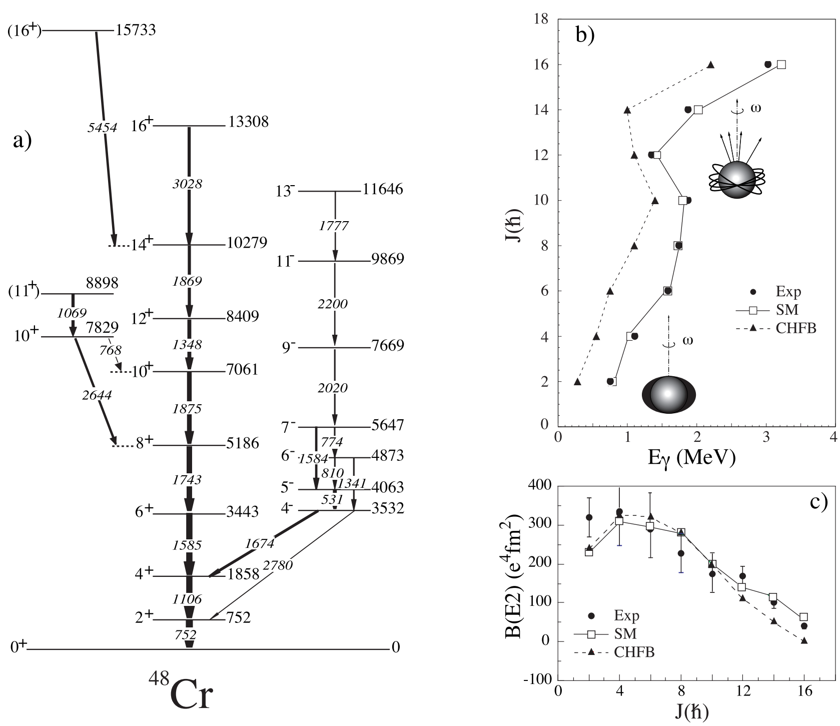

Fig. 1. Experimental level scheme (a), backbending plot (b) and deduced (from the lifetimes measurements) B(E2) values (c), for ^{48}Cr [5] (circles) compared with shell model (squares) and cranked Hartree–Fock–Bogoliubov (triangles) calculations from Ref. [1]

.

other hand, E1 transitions in $N = Z$ nuclei between $T = 0$ states are forbidden by isospin conservation. Based on the systematics of the intruder bands, that will be presented in Sect. 6, we had suggested a $K^\pi = 4^-$, assignment, sustained also by shell model calculations in which a nucleon is excited from the closed $d_{3/2}$ shell. We have now measured the polarization of this linking transition with the EUROBALL clover detectors, obtaining a pure non-stretched dipole transition (E1,$\Delta J = 0$). This fixes the definite spins and parity of the side band states and the degree of isospin mixing in ^{48}Cr could be now deduced. Both, the excitation energies and the B(E2) values deduced from the lifetime measurements of all these states, are extremely well described by the full pf spherical shell model calculations.

For the g.s. band, the agreement between experimental results and shell model calculation for both, the backbending plot (Fig. 1(b) and the deduced B(E2) values (Fig. 1(c) is very good. A complementary description can be also obtained for this nucleus in the framework of mean field approaches such as cranked Hartree–Fock–Bogoliubov (CHFB) [1]. One can see in the figures that the description of the electromagnetic properties is quite good (similar results have been obtained with Nilsson–Strutinsky calculations [6]), but the CHFB moment of inertia seems to be completely wrong. The point is that in $N = Z$ nuclei, valence protons and neutrons occupy the same orbits and therefore proton–neutron correlations can not be ignored [1, 6, 7]. Then, in calculations such as CHFB where the proton–neutron-pairing correlations are not taken into account, the moment of inertia is overestimated given a much more compressed level scheme. This has been proved [7] in two steps: using the Gogny interaction of the CHFB at the place of the KB3 in the shell model calculation one reproduces again the experimental values; on the other hand, neglecting the proton–neutron pairing contributions in the KB3 interaction, one obtains a similar overestimation of the moment of inertia with the shell model calculation. Therefore one can conclude that in these nuclei, proton–neutron interactions are essential to have a good description of the level scheme [7] . Another interesting point is that the B(E2) values decrease, at the backbending (10^+), to reach a minimum value at the band termination, telling us that the collectivity is decreasing with increasing angular momentum.

3. Backbending

From heavy nuclei we know that the backbending is originated by band crossings or particle alignment. In the $f_{7/2}$ mass region, we can use both shell model and CHFB to see what it is happening at the backbending that changes drastically the rotational behavior of the nucleus. It has been argued that it is the mixing of the $f_{7/2}$ and the $p_{3/2}$ orbits in the wave function, which gives rise to the quadrupole collectivity [1]. At the backbending, the occupation of the $f_{7/2}$ increases while that of the $p_{3/2}$, $f_{5/2}$ and $p_{1/2}$ decreases rapidly up to the band termination. At the band termination, the occupation of these last three excited orbits is almost zero and we have a fully aligned configuration with all the 8 particles in the $f_{7/2}$ orbital. These fractional shell occupancies were calculated with both shell model and CHFB in Ref. [1] giving similar results.

CHFB can also give us the behavior of the deformation parameters with spin, the $\beta \approx 0.26$ and $\gamma \approx 0$ values (a prolate axially symmetric nucleus) are almost constant up to the backbending and change at higher spin. This suggests that the nucleus is getting triaxial deformation at the backbending and then reaches a spherical shape at the band terminating state.

Recently, the backbending in ^{48}Cr has been also studied with other theoretical approaches: cranked Nilsson Strutinsky [6] as well as CHFB [8] predict a change of shape towards triaxial deformation. On the other hand, a band crossing between a deformed and a spherical structure has been predicted in the framework of the Generator Coordinate Method [9], yet projected shell model calculations [9], show a crossing between a 2-quasiparticle and a 4-quasiparticle band. We will elucidate from our experimental results which of these pictures is the right one for ^{48}Cr.

The excitation energies of the yrare states in Fig. 1(a) are well reproduced by shell model calculations. We have also seen that the deduced B(E2) values for the yrast states were also well described (Fig. 1(c)). We could not measure yet the lifetimes to deduce the B(E2) values for the yrare states because they are very weakly populated, and then we have to rely on the shell model calculation to get some conclusion. What we can say is that, from these calculations, the B(E2) values for the decay of the 10^+_2 on to the 8^+ is much smaller than that of the yrast 10^+_1 on to the 8^+; this could tell us that there is not a bandcrossing in this case. Although the yrare structure is rather collective (the intraband B(E2) values are quite constant) they do not seem to be the continuation of the g.s. band. Of course, we have to measure the lifetimes to give the last answer to this question.

An interesting point is the behavior of the wave functions in both yrast and yrare structures. The occupational numbers of the yrare states do not change significantly with the spin maintaining the slight collectivity even at high spins. At spin 16 we have an yrast fully aligned, non collective state and an yrare collective one. Then, it is energetically convenient for the nucleus to align particles along the rotational axis to generate angular momentum than continue with any collective motion above the backbending due to the fact that Coriolis and centrifugal forces, as pointed out above, are very strong in this rapid rotating light nucleus.

Another very good rotor in the $f_{7/2}$ shell is the nucleus ^{50}Cr that has 2 neutrons more than ^{48}Cr. In the backbending plot of Fig. 2(a) the ex-

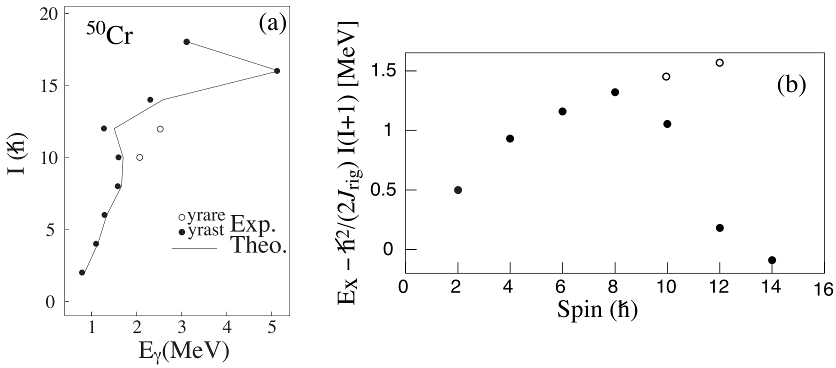

Fig. 2. (a) Experimental (circles) and shell model (line) backbending plot for ^{50}Cr; (b) the excitation minus rigid rotor energy for yrast (full circles) and excited (open circles) states.

perimental data are compared with the shell model calculation. The experimental yrare states are also plotted in the figure (white circles). The excitation energies of these states seem to continue the rotational ground-state sequence. In this case we have also measured the lifetime of the excited states. The deduced B(E2) value for the decay of the 10_2^+ on to the 8^+ is greater than that of the yrast 10^+ decay. This means that the g.s. band continues above the backbending but the yrast structure corresponds again to the alignment of particles. Which particles are aligning here will be discussed in Sect. 7.

4. Band termination phenomena

The band termination state is built when all the valence nucleons align to the maximum spin that can be constructed in a certain configuration. In all the nuclei we have studied in this mass region, the level schemes have been extended up to the band termination with all the valence nucleons in a pure $f_{7/2}$ configuration and, in several cases the level schemes have been extended beyond the band terminating state.

In the case of ^{50}Cr we have observed the band terminating state which corresponds to 6 neutrons and 4 protons fully aligned in the $f_{7/2}$ configuration, that is 14^+. Above this state we have seen many others states and in particular a second backbending at spin 18^+. A characteristics of band terminating states is that they are non collective.

A different and a very interesting case is the nucleus ^{52}Fe in which the maximum spin that can be constructed with 6 protons and 6 neutrons in the pure $(f_{7/2})^{12}$ configuration is 12^+. The yrast 12^+ state in this nucleus lies below the 10^+ state and constitutes an yrast trap. This nucleus has been an experimental challenge for many years because any attempt to study high spin states using fusion-evaporation reactions did not succeed because most of the flux was trapped at the 12^+ state and diverted to ^{52}Mn by β decay. Recently we were able to observe these states with Gasp. Full pf shell model calculations [10] reproduce with good accuracy the experimental data. This residual quadrupole collectivity in the 12^+ state, due to the mixing of the $f_{7/2}$ and $p_{3/2}$ components of the wave function, can be related to the energy inversion of the 10^+ and 12^+ states, which gives rise to the yrast trap. We have also performed calculations in the intrinsic frame considering a $K = 12$ prolate state in the Nilsson model. By further projecting this state onto good angular momentum, the overlap with the exact shell model wave function of the 12^+ state is of 90% [10]. This means that the description of the 12^+ state in terms of prolate deformation seems to be in agreement also with the shell model calculation.

We have measured recently the γ decay of the isomeric 12^+ state ($T_{1/2} = 45.9\,\mathrm{s}$) in ^{52}Fe with the on-line mass separator at the GSI [11]. In this experiment, the detection sensitivity limit has been improved by two orders of magnitude to that achieved in previous studies. We have established for the first time the γ de-excitation of the 12^+ isomer to the two previously [10] observed 8^+ states via E4 transitions of 597.1 and 465.0 keV. This gives a definite excitation energy of 6957.5 keV for the 12^+ state that was wrongly placed by 137 keV in previous β-decay studies. The deduced $B(\mathrm{E4})$ values are, however, very low compared to other values in this mass region. This could be consistent with the $K = 12$ assignment to the yrast trap because a big change of K value has to be done to connect this state with the 8^+ states lying below. This constitutes a strong test for the residual interaction. Detailed calculations in the shell model framework in order to reproduce the experimental findings are in progress [11].

5. $T = 1$ and $T = 0$ bands in $N = Z$ odd–odd nuclei

As it is well known, at variance with like-nucleon pairs which couple only to isospin $T = 1$, proton–neutron pairs can couple to both $T = 0$ and $T = 1$. In deformed odd–odd $N = Z$ nuclei in the $f_{7/2}$ shell, we have observed $T = 0$ and $T = 1$ structures at rather low excitation energies. There are also $T = 1$ structures in even–even $N = Z$ nuclei but they lie at much higher excitation energy. $T = 0$ rotational bands have been observed up to band termination in the most deformed odd–odd nuclei in this region: ^{46}V [12] and ^{50}Mn [13]. These nuclei have one proton–neutron pair added or subtracted to ^{48}Cr. The bandheads of these $T = 0$ bands have a very low excitation energy (less than 1 MeV) and the bands become yrast very soon. On the other hand, all odd–odd $N = Z$ nuclei in the $f_{7/2}$ shell have a $J = 0$, $T = 1$ ground-state but the g.s. band is non-yrast and cannot be followed up to high spin in our data. These rotational bands are isobarical analogue of those in ^{46}Ti and ^{50}Cr.

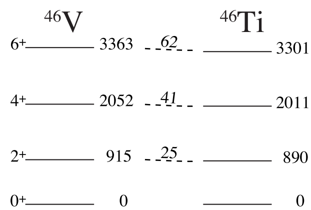

Fig. 3. $T = 1$ bands in the isobarical analogue ^{46}V and ^{46}Ti with the energy differences for each spin.

Due to the charge independent character of the nuclear force, the only difference between these two analogue $T = 1$ bands could come from the Coulomb interaction. In particular, the excitation energies of the $T = 1$ analogue states in ^{46}V are greater than those in ^{46}Ti up to spin 6^+ (Fig. 3). These Coulomb energy differences can be interpreted in terms of particle recoupling. We know that when a proton pair is coupled to $J = 0$ the overlap of the wave function and consequently, the Coulomb interaction get the maximum value. Then, in a rotating nucleus, when a proton pair changes from a $J = 0$ coupling to another J configuration, the repulsive Coulomb interaction decreases [14]. On the contrary, no Coulomb effects are expected for the alignment or recoupling of a neutron pair or a proton–neutron pair. Then, as the Coulomb field is repulsive, if proton pairs align in ^{46}Ti its level scheme will become more compressed than that of the odd–odd nucleus where a pn pair aligns. This interpretation in terms of nucleon pair recouplings can be also deduced from shell model calculations. The contributions to the energy of each state of the different pairing terms calculated in the shell model framework have been studied in Ref. [12]. The pairing interaction is well known to decrease with increasing spin due to the mechanism of particle alignment or recoupling. The most important contribution of the $T = 1$ pairing for ^{46}V arises from the pn term that decreases with increasing angular momentum while the contribution of the like-nucleon pairing remains almost constant. The opposite behavior is found for ^{46}Ti: both proton and neutron pairing correlations are decreasing with angular momentum while the $T = 1$ pn correlation remains constant. We can conclude that the Coulomb energy differences can be explain in terms of particle alignments, that is, like-particle alignment in ^{46}Ti and pn alignment in ^{46}V. We will return later to the Coulomb energy differences for mass 50 nuclei.

6. Intruder bands and shape coexistence

Intruder bands of non-natural parity come very low in excitation energy in the $f_{7/2}$ shell. What we observed is that for nuclei lighter than ^{48}Cr, that are filling the first half of the shell, these intruder structures are much more deformed than the g.s. bands due to the fact that more degrees of freedom come into play by exciting particles from the *sd* closed shell.

Coming back to the ^{46}V example [12], we see in Fig. 4(a) both signatures of the intruder band which are very regular, with a backbending around spin $J = 10$, and can be described in terms of a Nilsson coupling as the two signatures of a $K = 0^-$ band. These structures can be reproduced very well with the spherical shell model in which only one particle is allowed to jump from the $d_{3/2}$ orbit to the fp main shell (Fig. 4(b) and (c)). This configuration rules most of the intruder rotational bands we have studied. In particular for ^{46}V we have observed both signatures up to the band termination in the $(f_{7/2})^7 \otimes (d_{3/2})^{-1}$ configuration.

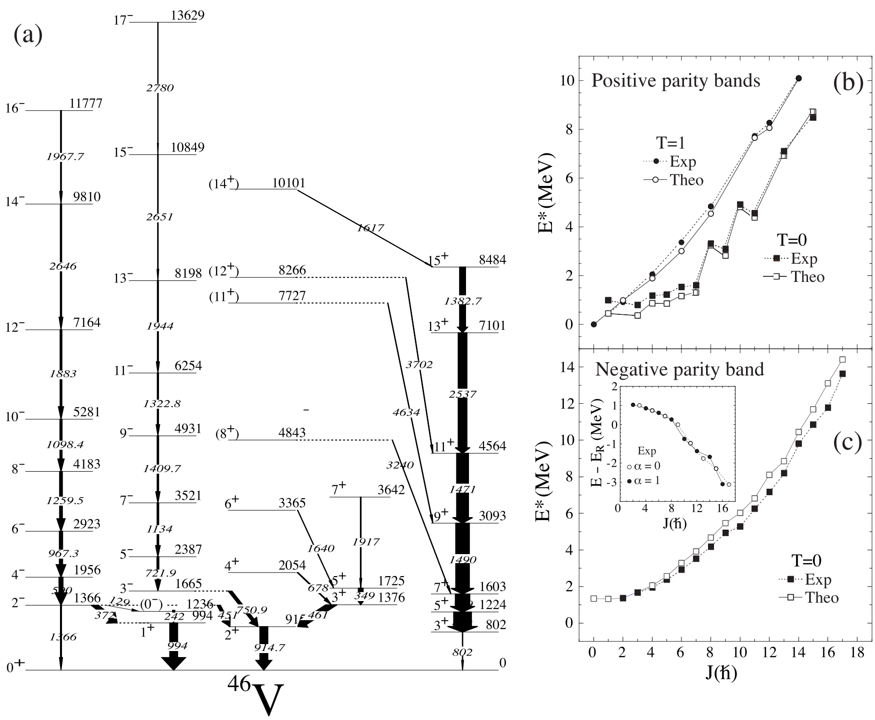

Fig. 4. Level scheme (a) and the experimental excitation energy vs. spin plot for the positive (b) and negative (c) parity bands of ^{46}V (black symbols) compared with shell model calculations from Ref. [12] (open symbols)

An interesting point is that we can speak in these nuclei about shape coexistence. In fact, the behavior of the negative parity band (Fig. 4(c) is consistent with a well deformed structure, a regular rotational band with a backbending around 10. On the other hand, the $T = 0$ positive parity band structure (Fig. 4(b)) shows very low deformation. We have observed shape coexistence in most of the nuclei that are filling the first half of the $f_{7/2}$ shell, in which normally the natural parity structures are much less deformed than those of the intruder bands. This shape coexistence is sustained by the lifetime measurements we have performed in some of these systems.

We have observed non-natural bands up to high spin, in ^{43}Sc, ^{44,46}Ti, ^{46,47,48}V and ^{48,49}Cr.

7. Isobaric analogue rotational bands in mirror $T = 1$ nuclei

The study of isospin symmetry in mirror nuclei or isobaric analogue multiplets has been limited to light nuclei and low spins. It is now possible to extend considerably these studies to higher masses and angular momenta to investigate this symmetry at high angular frequencies. The odd mass mirror nuclei of mass $A = 47, 49, 51$ have been studied up to the band termination in the last few years [14–16]. Very interesting features have been found as for example that the experimental Coulomb Energy Differences (CED) constitute a fingerprint for nucleon alignment at the backbending.

Now, if we want to extend this investigation to $T = 1$ isobaric analogue nuclei, we have to study the isospin symmetry at high angular momentum, but then, as we have seen before in the case of an isobaric multiplet, it is not possible to extend for the odd–odd nucleus the $T = 1$ bands up to high spin because the $T = 0$ structures become yrast very soon and we have to limit our investigation to quite low spins. Therefore, if we have to look for this isospin symmetry at the backbending we have to study the mirror symmetry between even–even nuclei ($N = Z \pm 2$). In these even–even nuclei there are not blocking effects and, *a priori*, it is more difficult to understand which type of particles will align in the backbending. One of the better rotors in the $f_{7/2}$ shell is the nucleus ^{50}Cr, which presents a first backbending around spin 10^+ [17]. Then, one of our candidates was ^{50}Fe, in which no γ transitions were known before our experiment. We have recently performed this experiment at Legnaro [18]. γ rays were detected with EUROBALL, Isis silicon ball and the Neutron Wall.

We have observed a rotational band structure up to the 11^+ state that can be compared with the corresponding g.s. band of the $N = Z + 2$ mirror, ^{50}Cr (Fig. 5(a). The cross section for ^{50}Fe was more than 4 order of magnitude less that the corresponding to ^{50}Cr.

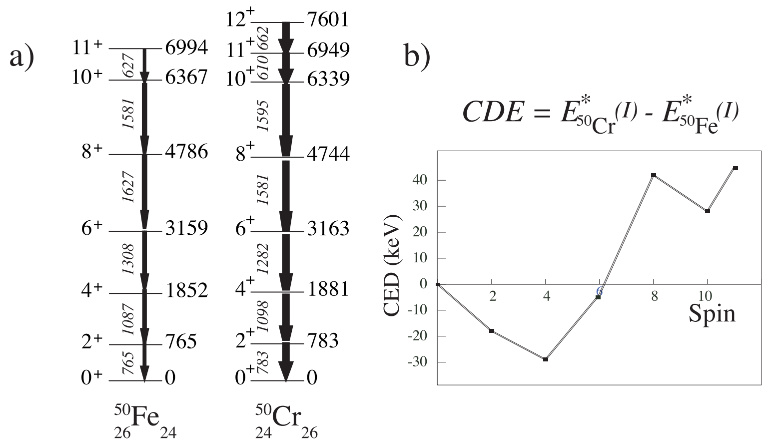

Fig. 5. Comparison of the g.s. bands (a) and the Coulomb difference energies (b) for the $A = 50$ mirrors ^{50}Cr and ^{50}Fe.

In Fig. 5(b) the behavior of the experimental Coulomb energy difference as a function of the spin is shown. The jump at spin 8^+, in the backbending region, can be related to a change in the alignment of a neutron pair in ^{50}Fe while a proton pair aligns in ^{50}Cr; at spin 10^+ a second alignment of the other type of like-nucleon pairs occurs, a proton pair aligns in ^{50}Fe while a neutron pair does it in ^{50}Cr. The data is qualitatively well described by the cranked shell model calculations of Ref. [19] that agrees with our interpretation.

8. Conclusions

At low spin, nuclei in the middle of the $f_{7/2}$-shell show collective behaviour, and at increasing angular momentum single particle degrees of freedom are observed as, for example, alignment of the nucleon spins along the rotational axis giving rise to backbending and band-termination phenomena. These effects have been illustrated and discussed in several results obtained with the high efficiency experimental facilities available for nuclear spectroscopy studies. The possibility of describing these systems with both exact shell model calculations and deformed mean field models allows for complementary views of the different properties.

It has been shown that proton–neutron correlations are essential to reproduce the level schemes of $N \approx Z$ nuclei.

The study of the 12^+ yrast trap in ^{52}Fe put in evidence the collective character of this state and its γ decay by E4 transitions has been measured for the first time. The weak B(E4) values could confirm the previous $K = 12$ assignment.

Non-natural parity bands in this mass region can be described as $(f_{7/2})^{n+1}\,(d_{3/2})^{-1}$ configurations. These structures are much more deformed than the g.s. bands in most of the cases.

Finally, we have shown that Coulomb energy differences in isobaric analogue rotational bands are the fingerprints of the type of nucleons that are aligning at the backbending.

This work is the result of a big and fruitful collaboration with many colleagues to whom I have to thank.

REFERENCES

[1] E. Caurier *et al., Phys. Rev. Lett.* **75**, 2466 (1995).
[2] T. Otsuka *et al., J. Phys. G* **25**, 699 (1999).
[3] G. Martinez-Pinedo *et al., Phys. Rev.* **C54**, R2150 (1996).
[4] S.M. Lenzi *et al., Z. Phys.* **A354**, 117 (1996).
[5] F. Brandolini *et al., Nucl. Phys.* **A642**, 347 (1998).
[6] A. Joudagalvis *et al., Phys. Lett.* **B477**, 66 (2000).
[7] A. Poves *et al., Phys. Lett.* **B430**, 203 (1998).
[8] T. Tanaka *et al., Phys. Rev.* **C58**, 2765 (1998).
[9] K. Hara *et al., Phys. Rev. Lett.* **83**, 1922 (1999).
[10] C.A. Ur *et al., Phys. Rev.* **C58**, 3163 (1998).
[11] A. Gadea *et al.*, Proc. of the Pingst 2000 workshop, Lund (2000).
[12] S.M. Lenzi *et al., Phys. Rev.* **C60**, 021303 (1999).
[13] C.E. Svensson *et al., Phys. Rev.* **C58**, R2621 (1998).
[14] J.A. Cameron *et al., Phys. Lett.* **B235**, 239 (1990).
[15] M.A. Bentley *et al., Phys. Lett.* **B437**, 243 (1998).
[16] J. Ekman *et al.*, Proc. of the Pingst 2000 workshop, Lund (2000).
[17] S.M. Lenzi *et al., Phys. Rev.* **C56**, 1313 (1997).
[18] N. Marginean *et al.*, to be published.
[19] J.A. Sheikh *et al., Phys. Lett.* **B443**, 16 (1998).